

Research article

## **Analysis of force fluctuation in order to determine structural defects in hot strip rolling mills**

Yaser Jahangardy<sup>a</sup>, Mohammad Reza Forouzan<sup>a\*</sup>, Majid. Rostamipour<sup>b</sup>

<sup>a</sup>Department of Mechanical Engineering, Isfahan University of Technology, Isfahan, 84156-83111, Iran

<sup>b</sup>Mobarakeh Steel Company, Isfahan, Mobarakeh, 84815-1, Iran

Received 23 September 2012    Revised 22 December 2012    Accepted 25 December 2012

### **Abstract**

Structural defects of the mill have considerable effect on the product quality in conventional strip rolling. Since the working rolls are in direct contact with the product, geometrical deviation of them is the most effective parameter on the product quality. In this paper a dynamic model for evaluating mill response to different major structural defects for hot strip rolling is presented for the first time. The model has two main sub-models; the stand elastic model and the strip rolling plastic model. Roll surface flattening and the material hardening due to strain and strain rate are the main sources of the nonlinearities in the mill and the rolling process sub-models respectively. In the presented procedure, in each step, both the models were linearized around the steady state working point and the stiffness matrix was updated in each step. The SIMULINK tool of the MATLAB software was employed to simulate the interactions of the sub-models. The model is able to undertake seven stands in a tandem four-high mill simultaneously. Defects such as ovality and eccentricity of work roll and backup roll have been modeled and the simulation results are in very good agreement with data gathered from an industrial mill data logger.

©2012 Usak University all rights reserved.

**Keywords:** Hot strip rolling, forced vibration, structural defect

### **1. Introduction**

Mill stand vibrations limit the rolling speed, degrade product quality and sometimes damage the mill. Forced vibration is one of the most important phenomenon that can be occurred in hot strip rolling mills and blemish some equipment of mill stand and reduce the strip quality. In order to control and suppress these vibrations, a comprehensive understanding of the rolling dynamic nature both in the strip plastic deformation and mill stand vibration are required. To study the phenomenon of rolling mill vibration, an appropriate model of the rolling process as well as that of the mill stand must be established at first. Then by coupling them, rolling mill vibration can be investigated [1].

One of the most comprehensive analyses of the flat rolling process is due to Orowan [2]. Unlike other researchers, Orowan discarded the assumptions of constant yield stress during the rolling pass, slipping over the whole arc of contact and homogeneous compression. Many researchers since then have been trying to simplify the model

\*Corresponding author: Tel: +98 -311- 3915235, Fax: +98 -311- 3912628  
e-mail: [forouzan@cc.iut.ac.ir](mailto:forouzan@cc.iut.ac.ir)

proposed by Orowan, Bland and Ford [3, 4] and Sims [5, 6] used simplified assumptions and proposed analytical expressions of pressure distribution, roll torque and roll force.

Afterward many mathematical models for the plastic deformation of plate during rolling process have been established with various degrees of simplification or limitation. Conventional models such as those proposed by Alexander [7], Christensen et al. [8], Gunasekera and Alexander [9], Lalli [10], Venter and Abd-Rabbo [11], Freshwater [12] offer some accurate estimation of the rolling parameters, but are not suitably applicable in dynamic analysis.

Plusty et al. [13] explained the dynamic behavior of self-excited vibrations in rolling. They undertook the change in the contact length between rolls and the strip during vibration and calculated the resulting rolling force change. They also established a criterion for system instability. Hu [1] further extended the analysis by using an enhanced rolling process model. Afterward Hu and Ehman [14] proposed a linear dynamic rolling process model that relaxes many of the assumptions of the rolling process models reported in the literature. The model was adapted for cold rolling. Yan et al. [15] studied a serious vibration phenomenon which can occur in F2-F4 stands during rolling thin gauge or high strength strip. Yildiz et al. [16] proposed one-dimensional hot rolling mill model using for looper control analysis. Fan et al. [17] established the horizontal roller friction flutter model according to the nonlinear stick-slip friction characteristic of rolling interface. They also presented the work roll "jump vibration" model of horizontal direction with unbalanced force caused by spindle. Besides they proposed the nonlinear dynamic model of rolling mill vertical vibration by introduction to Duffing oscillator and the parametrically excited stiffness [18].

The second base of any rolling vibration model is the structural model [14], which is the elastic model of the mill stand. Several models have been proposed for simulating mill structure, but it has been shown that the simple 2D models have proper accuracy in modeling the mill. These models are consist of linear springs and lumped masses which vibrate perpendicular to the rolling direction. For instance Yarita et al. [19] represented a four-high mill as a vibration system with four degrees of freedom. Chefneux et al. [20] also used a linear lumped parameter system with all the masses vibrating along the same principal direction to model a four-high mill. Stiffness due to elastic deformation of the screw down and stand, elastic contact between the backup roll and the work roll, and the elastic deformation of the work roll and the strip were all represented by linear springs [19, 20]. Sun et al. [21] has established the forced transverse vibration model of rolls for four-high cold rolling mill. The work roll and backup roll has been considered as elastic continuous bodies that were joined by a Winkler elastic layer. They have shown that the influence of moment of bending rolling force on the vibration of work roll is related with the bending roll force. Lü et al. [22] used the Least squares method to identify the hot rolling mill abnormal vibration model on the basis of foregoing analysis. . Yan et al. [23] have built a simulation model of the F3 mill's main drive system using MATLAB software. They analyzed the dynamic characteristics of the system during biting and exceptional vibration.

In this paper the dynamic model of the hot strip rolling is presented for the first time. This model is based on dynamic model proposed by Hu et al. [14] for self-exiting vibration in cold rolling. But with two main differences; first, it has adopted for hot rolling vibration by undertaking strain rate effects and second it undertakes effect of forced vibration due to structural defects. The model has two main sub-models, the stand elastic

model and the strip rolling plastic model. Roll surface flattening, and the material strain rate hardening are the main sources of the nonlinearities in the mill and the rolling process sub-models respectively. Both of the sub-models are linearized around the steady state working point and their interaction is simulated using the SIMULINK tool of the MATLAB software. The effects of rolls defects on force fluctuation are investigated.

## 2. The Dynamic Rolling Model

### 2.1. Single-Stand Rolling Model

Fig. 1 shows simplified block diagram of a single rolling stand proposed by Hu and Ehman [14]. In this figure  $G_p$  and  $G_s$  represent the transfer functions of rolling plastic process and stand elastic model respectively.  $G(s)$  represents transfer function of whole the stand model where;

$$G(s) = (I + G_s)(I - G_p G_s)^{-1} G_p \tag{1}$$

The input vector  $r$  contains all the parameters coming from outside the stand and the output vector  $y$  contains all those affecting upstream and downstream stands. Input and output vectors of the rolling process  $G_p$  and structure model,  $G_s$  are shown as  $u_p, y_s, u_s,$  and  $y_p$  respectively, All functions are linearized around the steady state point. Therefore input or output vectors mainly contain divisions from steady state condition.

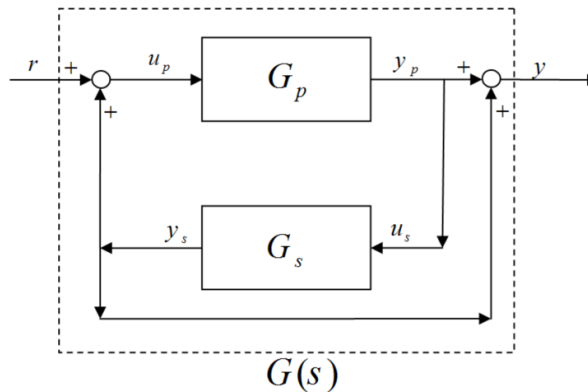


Fig. 1 Block diagram of single-stand chatter model [14]

### 2.2. Rolling Process Model

In Fig. 1, the components of the input vector  $u_p$  for rolling process are the deviations of following parameters; strip backward and forward stress tensions ( $d\sigma_{x,1}, d\sigma_{x,2}$ ), strip input thickness,  $dh_1$ , horizontal displacement of the center of work roll,  $dx_c$ , central roll gap,  $dh_c$ , and the work the roll peripheral velocity,  $dv_r$ . These parameters are shown in Fig. 2.

$$u_p = [d\sigma_{x,1} \quad d\sigma_{x,2} \quad dh_1 \quad dx_c \quad dh_c \quad dv_r]^T \tag{2}$$

Deviation on inputs leads to deviation of outputs related to the rolling process transfer function;

$$y_p = G_p u_p \tag{3}$$

Where

$$y_p = [df_x \quad df_y \quad dM \quad du_1 \quad du_2]^T \tag{4}$$

$y_p$  is the extended output vector,  $f_x$  and  $f_y$  are the horizontal and vertical components of the rolling force,  $M$  is the rolling torque, and  $u_1$  and  $u_2$  are the strip entry and exit velocities, The transfer function  $G_p$  is a 5×6 matrix which its components can be found in [14] for cold strip rolling. Horizontal component of rolling force is negligible comparing its vertical part. Consequently it has a very small effect on fluctuation of the vertical force or displacement. Therefore all horizontal factors in input and output vectors i.e.  $dx_c$  and  $df_x$  are assumed to be zero [1, 13-19].

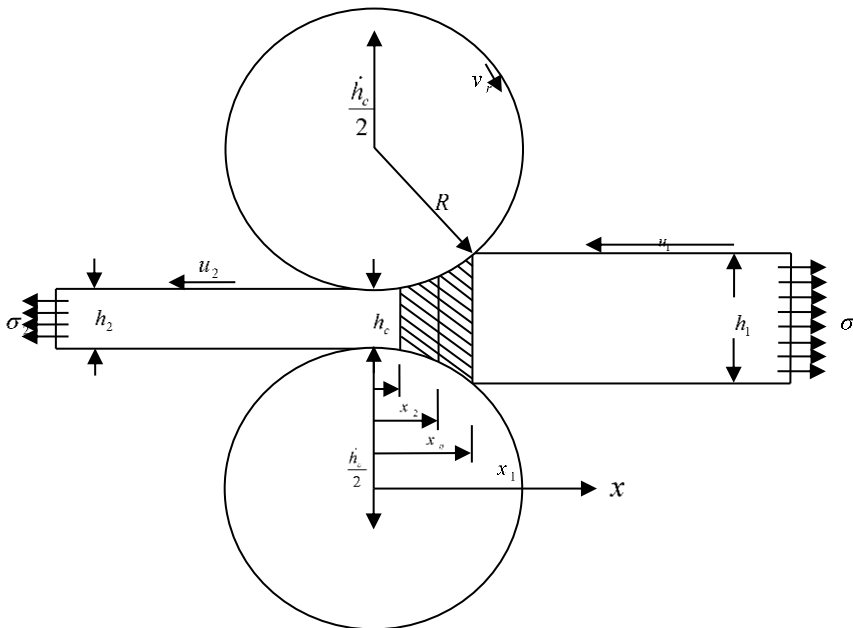


Fig. 2 Strip and rolls geometry

### 2.3. Implementation for Hot Strip Rolling

The main challenge on implementing the above model for hot strip rolling is the dependency of the components of the transfer function matrix to the deformation strain rate due to strain rate dependency of the material yield stress in high temperatures. Shida's equation is of the most common constitutive equations which is using in rolling force prediction in hot strip rolling plants [25]. Shida's equation is given as follows:

$$\sigma_{shida} = \sigma_d (C, T) f_w (\varepsilon) f_r (\dot{\varepsilon}) \tag{5}$$

where

$$\sigma_d = 0.28 \exp\left(\frac{5}{T} - \frac{0.01}{C + 0.05}\right)$$

$$T [k] = \frac{T [^\circ c] + 273}{1000}$$

$$f_w (\varepsilon) = 1.3 \left(\frac{\varepsilon}{0.2}\right)^n - 0.3 \left(\frac{\varepsilon}{0.2}\right)$$

$$n = 0.41 - 0.07[c]$$

$$f_r (\dot{\varepsilon}) = \left(\frac{\dot{\varepsilon}}{10}\right)^m$$

$$m = (-0.019c + 0.126)T + (0.076C - 0.05)$$

where [c] is the steel carbon percentage,  $\varepsilon$  is the strain,  $\dot{\varepsilon}$  is the strain rate,  $m$  and  $n$  are the constants found from experiment.  $\sigma_{shida}$  is the yield stress and  $T$  is the strip temperature in Kelvin. Shida estimated the first term in Eq. 5 for the temperature domain between 700 and 1200 Celsius degree [25]. It is important to express a mean value for effective strain and strain rate for whole the elements in the roll gap.

$$\bar{\varepsilon}_{eff} = \frac{4}{\sqrt{3}x_1} \left[ x_1 - \sqrt{R_w h_{c1}} \arctan\left(\frac{x_1}{\sqrt{R_w h_{c1}}}\right) \right] \tag{6}$$

where  $x_1$  is the entry position of the strip,  $R_w$  is the work roll diameter and  $h_{c1}$  is the entry position roll gap spacing. With the same definition, the effective strain rate can be derived as follow;

$$\dot{\bar{\varepsilon}}_{avr} = \frac{2}{\sqrt{3}x_1} \frac{(u_1 + u_2)}{2} \ln\left(\frac{h_1}{h_{c1}}\right) + \left(\frac{\dot{h}_1 R_w}{\sqrt{h_{c1} R_w}}\right) \arctan\left(\frac{x_1}{\sqrt{h_{c1} R_w}}\right) \tag{7}$$

where  $\dot{h}_1$  is the rate of entry position roll gap spacing.

#### 2.4. Structural Dynamic Model

Structural dynamic model of the mill stand consists of two parts: a linear vibration model and a rotational vibration model. In this study Uni-Directional symmetric Multi-Modal structure model has been used which is presented in Fig. 3 [26]. In this figure the rolling process is considered in its steady state condition and so linear spring and dampers could be defined not only between the backup roll and the stand foundation ( $K_b, C_b$ ) but also

between work roll and the backup roll ( $K_w, C_w$ ). Accordingly;

$$\begin{cases} M_w \ddot{y}_w + C_w (\dot{y}_w - \dot{y}_b) + K_w (y_w - y_b) = w df_y \\ M_b \ddot{y}_b + C_b \dot{y}_b + K_b y_b = C_w (\dot{y}_w - \dot{y}_b) + K_w (y_w - y_b) \end{cases} \quad (8)$$

where  $df_y$  is deviation of rolling force per unit strip width ( $w$ ) from its steady state value. Hu [14] supposed that deviation in work roll radius could be ignored due to  $df_y$ . That leads to a simple conclusion for symmetric vibration modes;

$$y_c = \frac{dh_c}{2} \quad (9)$$

where  $h_c$  is the roll gap spacing. Consequently by applying the Laplace transform in the frequency domain we have;

$$\frac{dH_c(s)}{df_y(s)} = 2w \frac{M_b s^2 + (C_w + C_b)s + (K_w + K_b)}{D_s(s)} \quad (10)$$

Similarly dynamic of drive shafts can be modelled by a simple one degree of freedom system [1];

$$I \ddot{\theta} + B \dot{\theta} + k_r \theta = -w dM \quad (11)$$

where  $I$  is the equivalent moment of inertia of the rolls,  $B$  is the rotational damping constant caused by the thin oil film in the roll bearings, and  $k_r$ , is the rotational spring constant of the drive shaft. It is remarkable that  $k_r$  is usually very small due to the relatively high radius-to-width ratio of the roll and can sometimes be neglected without giving up much accuracy. The transfer function between the variation of roll velocity and the variation of torque can be written as:

$$\frac{dV_r(s)}{dM(s)} = \frac{-wR s}{Is^2 + Bs + k_r} \quad (12)$$

where  $v_r$  is the work roll parameter speed and  $R$  is its radius.

## 2.5. Multi-stand Rolling Model

Interstand tension and mass transfer between stands are the main factors that transmit vibrations from one stand to the others. Hu [14] established a dynamic model appropriate with multiple-stand tandem mills. The model is presented in Fig. 4. The single-stand rolling model for stand  $i$  is represented by  $G_i(s)$ . Signals from upstream and downstream stands are passed into  $G_i(s)$  through the transport matrix  $T_i$ .

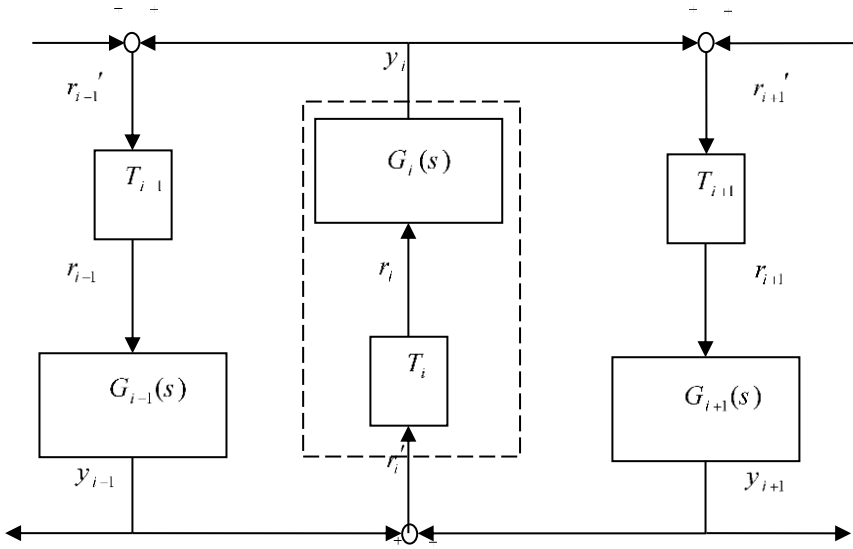


**Fig. 4** Block diagram of multi-stand rolling model [14]

The input vector  $r'$  in Fig. 4 is;

$$r'_i = [du_{2,i-1} \quad du_{1,i-1} \quad du_{c,i-1}] \tag{13}$$

$T_i$  adjusts forward and backward tensions of the current stand ( $i$ ) based on rolling speeds of preceding ( $u_{i-1}$ ) and subsequent ( $u_{i+1}$ ) stands by means of matrix  $H$ . Components of  $H$  are the results of integration from Hooke's law in the frequency domain.

$$H_i = \begin{bmatrix} \frac{-E}{L_{i-1}s} & 0 & 0 \\ 0 & \frac{E}{L_i s} & 0 \\ 0 & 0 & 0 \end{bmatrix} \tag{14}$$

Where  $L_i$  is the distance between stands  $i$  and  $i+1$ . On the other hand waves printed on the strip surface from the former stand determine the input strip thickness variation in the current stand after a time delay of  $\Delta_i = L_{i-1}/u_{2,i-1}$  which can be considered by defining matrix  $D_i$  ;

$$D_i = \begin{bmatrix} 0 & 0 & 0 \\ 0 & 0 & 0 \\ 0 & 0 & e^{-s\Delta_i} \end{bmatrix} \tag{15}$$

The expression for  $T_i$  can then be written as:

$$T_i = (I + H_i G_i)^{-1} (H_i + D_i) \tag{16}$$

### 2.6. Mathematical Model for Structural Defects

Variation in the central roll gap as well as variation in work roll radius determines the variation in the position of the work roll center.

$$dY_w = \frac{dh_c}{2} + dR_w \tag{17}$$

Similarly variation in the position of the backup roll center could be related to the roll gap, the work roll and the backup roll geometry;

$$dY_b = \frac{dh_c}{2} + dD_w + dR_b \tag{18}$$

Radius of an eccentric roll varies with a frequency as the rotational frequency. Rolls which are positioned eccentric from rotation axes or ground eccentric are of the examples of eccentric rolls. Note that eccentricities due to roll elastic deflections do not change stand rolls position. Radius variation for an eccentric roll which is rotating with frequency  $\omega$  approximately can be expressed as follows;

$$\Delta R = e (1 + \cos(\omega t + \theta)) \tag{19}$$

Where  $e$  is the roll eccentricity,  $t$  is the time and  $\theta$  is the start eccentricity angle related to the base line. Perimeter of a circular roll may practically deviates from its ideal shape. Deviation curve may be approximated by a cosine function with a wave length proper fraction of the roll perimeter. The most usual rolls are oval section rolls with periodic deviations. These deviations are repeated two times in the roll perimeter, so roll radius deviation appears with a frequency twice rotational frequency of the roll;

$$\Delta R = \left( \frac{b-a}{4} \right) (1 + \cos(2\omega t + \theta)) \tag{20}$$

where  $b$  and  $a$  are the larger and the smaller diameters of the oval section. By substituting Eqs. 17, 18 and 20 into Eq. 8 and using Laplace transformation, the displacement of work roll center for oval work roll and backup roll, can be derived as;

$$Y_w = \frac{N}{D(s)} \left( \frac{C_w K_w (d+z) S + K_w^2 (d+z)}{N} - K_w (d+z) + wdf_y \right) \tag{21}$$

$$D_s(s) = M_w M_b s^4 + [M_w C_b + (M_w + M_b) C_w] s^3 + [M_w K_b + (M_w + M_b) K_w + C_w C_b] s^2 + (C_w K_b + C_b K_w) s + K_w K_b \tag{22}$$

$$N = (M_b S^2 + (C_b + C_w) S + (K_b + K_w)) \tag{23}$$



$$d = \left( \left( \frac{b-a}{4} \right) \left( \frac{1}{s} + \cos \theta \left( \frac{s}{s^2 + 4\omega^2} \right) \right) - \sin \theta \left( \frac{2\omega}{s^2 + 4\omega^2} \right) \right) \quad (24)$$

$$Z = \left( \left( \frac{b'-a'}{4} \right) \left( \frac{1}{s} + \cos \phi \left( \frac{s}{s^2 + 4\omega'^2} \right) \right) - \sin \phi \left( \frac{2\omega'}{s^2 + 4\omega'^2} \right) \right) \quad (25)$$

$\phi$  and  $\theta$  are the start ovality angle related to the base line of backup roll and work roll respectively. Parameters with prim are belong to backup roll.

### 3. Implementation on SIMULINK

The model was constructed in the SIMULINK of MATLAB software. Simulation of the hot rolling forced vibration has been done by considering different structural defects. Fig. 5 shows the total model of the simulation and how the seven stands are connected to each other. As can be seen, this model involved 8 boxes which the first models the strip feeder and the others model the seven tandem stands. The strip feeder is named pay off reel and is a simple device which is used to set back tension in the first stand. Fig. 6 shows the components of one stand model. Any STAND model consists of three main parts which are named "Transport", "Connection" and "Stand". Role of the transportation and the connection parts is to arrange information coming from upstream and downstream stands to be applicable for the current stand. On the other hand the outputs of one stand affect its inputs, so these two parts include this effect. The box stand models rolling process based on the theory discussed in parts 2.1 to 2.3.

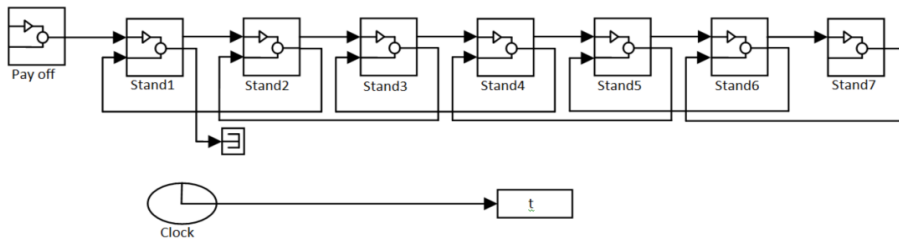


Fig. 5 Seven stand simulation of hot rolling mill vibrations at SIMULINK software

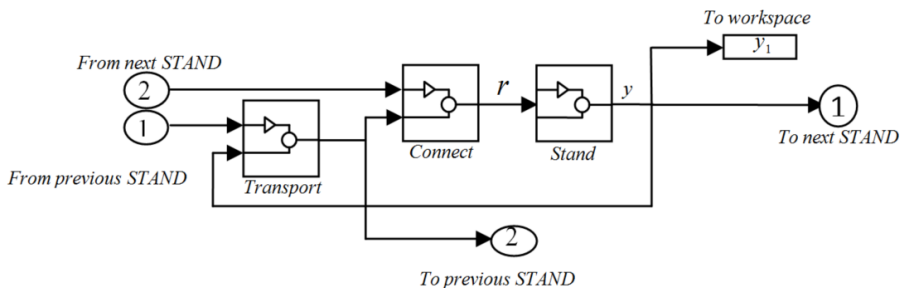


Fig. 6 One STAND vibration simulation of hot rolling mill with its transportation and connection blocks

## 4. Results and Discussion

### 4.1. Experimental Data

To compare simulation results with real experimental data, data from an industrial hot rolling production line of Mobarakeh Steel Company (MSC) were collected. The mill under study contains 4-high 7-stand hot strip mill and has benefit of an online data logger, which can collect many of process parameters such as rolling force and roll gap fluctuations at all stands. Frequency of data recording in the data logger is 100 Hz. Table 1 contains specification of the hot strip rolling machine in the MSC. Analyses present here are based on a typical rolling program which its specifications are presented in Table 2.

**Table 1**

Specification of hot strip rolling machine, WR: Work roll, BR: Back up roll

BR mass (ton)	WR mass (ton)	BR diameter (cm)	WR diameter (cm)	Distance between stands (cm)	Plate width (cm)
30	8	140	70	550	125

**Table 2**

Strip dimensions and rolling specification under study

Stand	1 <sup>st</sup>	2 <sup>nd</sup>	3 <sup>rd</sup>	4 <sup>th</sup>	5 <sup>th</sup>	6 <sup>th</sup>	7 <sup>th</sup>
Plate thickness at entry (mm)	30.00	19.42	11.00	8.80	6.00	4.45	3.60
Plate thickness at exit (mm)	19.42	11.00	8.80	6.00	4.45	3.60	3.00
Entry velocity (m/s)	1.20	1.85	3.27	4.09	6.00	8.09	10.00

### 4.2. Defect Detection Procedure

Fast Fourier Transform (FFT) is a powerful analytical tool that is commonly used for detecting periodicity patterns and tandem repeats. It is used for comparing experimental and simulation data. Fig. 7 shows result of applying standard FFT to the force fluctuation data from data logger in the 5<sup>th</sup> stand of the 7 stands hot rolling MSC mill. Three strong peak points are picked and considered in this figure. These points are belonging to the defects on the mill or the entering strip. Other peaks which are not as strong as these three peaks are due to other kind of defects such as bearing defects and so are not marked in Fig. 7.

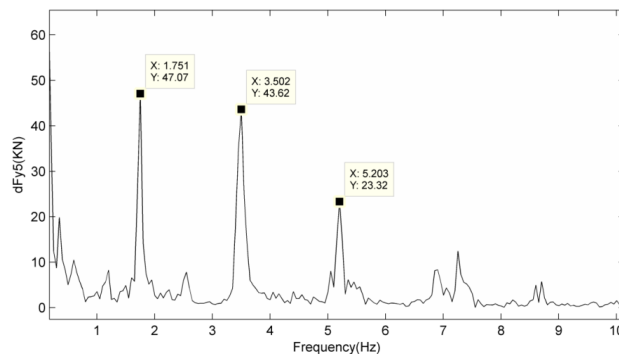


**Fig. 7** FFT of experimental force fluctuation data in the 5<sup>th</sup> stand

Using the code discussed in the previous section rolling force fluctuation could be simulated by modeling defects on the mill. There are two main unknowns for any defect; its location and its amplitude. For simple defects such as roll eccentricity or ovality it is easy to find the location of the defect by comparing rotational frequency of any roll with the force fluctuation frequency. But determining defect amplitude needs some try and error. For start, force fluctuation is determined as a function of time using the simulation program assuming an arbitrary initial value for the defect amplitude. Then the graph maps to the frequency domain by means of taking FFT. From FFT diagram, force fluctuation amplitude could be compared with the amplitude of the force fluctuation from data logger FFT. Now the next defect amplitude could be judged. This loop will be continued until force fluctuation amplitude from simulation converges to its similar value from the data logger.

Three different defects are distinguishable in Fig. 7. Fig. 8 shows result of rolling force fluctuations in the 5<sup>th</sup> stand due to simulation of mentioned roll defects in Table 3.

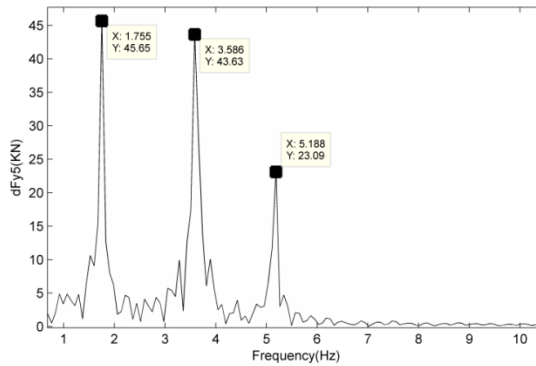


**Fig. 8** Result of rolling force fluctuations in the 5<sup>th</sup> stand due to simulation of mentioned roll defects in Table 3

As can be seen from this figure by implementing the mentioned defects in the simulation, the frequency and amplitude of rolling force fluctuation in 5<sup>th</sup> stand is the same as of real experimental data which is shown in Fig. 7. Using a similar procedure in analyzing rolling force fluctuation of the 6<sup>th</sup> stand two other defects on the 6<sup>th</sup> and 7<sup>th</sup> stands are detected. These defects are introduced in Table 4.

**Table 3**

Detail of defects considered in Fig. 7. E: Eccentricity, O: Ovality, WR: Work roll, BR: Back up roll, S: Stand

Frequency (Hz)	1.755	3.586	5.188
Defect amplitude (mm)/location	0.09-E-WR-2 <sup>nd</sup> S	0.02-E-WR-5 <sup>th</sup> S	0.035-E-WR-7 <sup>th</sup> S
	0.05-E-BR-5 <sup>th</sup> S	0.06-O-WR-3 <sup>rd</sup> S	0.065-O-WR-4 <sup>th</sup> S

**Table 4**

Predicted defects based on rolling force fluctuations in 6<sup>th</sup> stand. E: Eccentricity, O: Ovality, WR: Work roll, BR: Back up roll, S: Stand

Frequency (Hz)	2.747	4.425
Defect amplitude (mm)/location	0.035-E-BR-7 <sup>th</sup> S	0.033-E-WR-6 <sup>th</sup> S

Depth to huge amount of experimental results reserved on the data logger the accuracy of the method could be checked and verified easily. Fig. 9a and Fig. 10a show the simulation results of rolling force fluctuations in 6<sup>th</sup> and 7<sup>th</sup> stands due to defects predicted based on rolling force fluctuation in 5<sup>th</sup> and 6<sup>th</sup> stands i.e. defects mentioned in Table 3 and Table 4. Results of these figures in comparison with the results of Fig. 9b and Fig. 10b which are related to the data logger in the 6<sup>th</sup> and 7<sup>th</sup> stands shows very good agreement between empirical and simulation results.

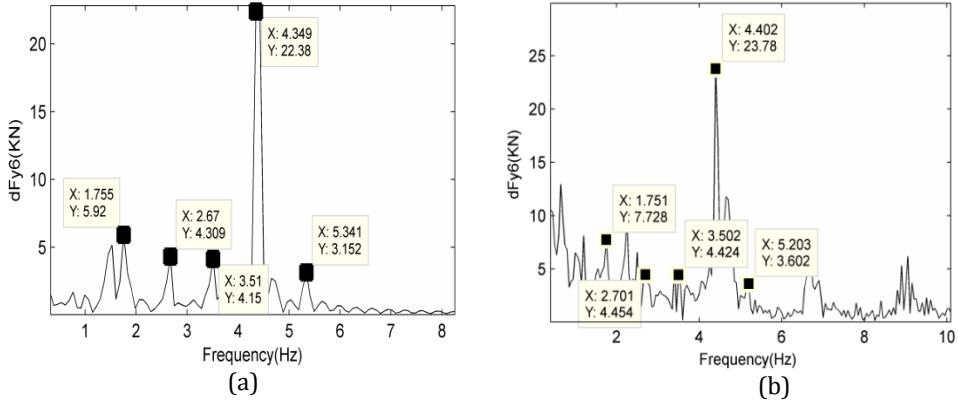


**Fig. 9** FFT of force fluctuations for 6<sup>th</sup> stand (a) simulation (b) data logger

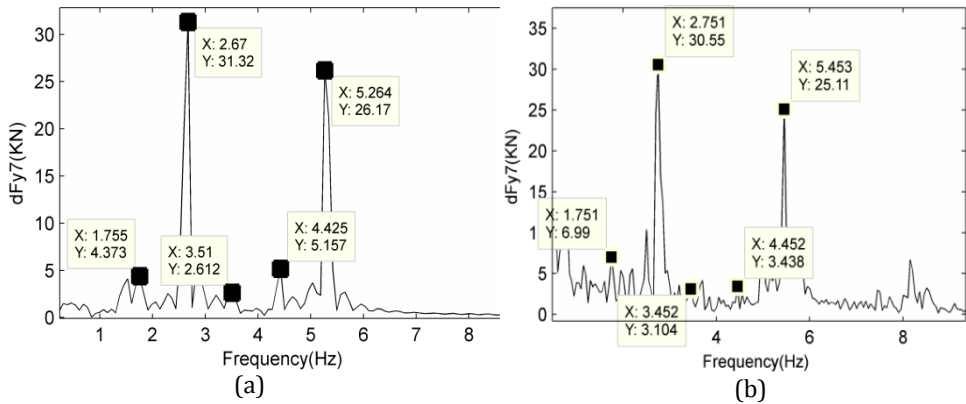


**Fig. 10** FFT of force fluctuations for 7<sup>th</sup> stand (a) simulation (b) data logger

In the above example stands number 5 and 6 were used to detect the defects, while the stand number 7 was used to verify the detected defects. We name the 5<sup>th</sup> and 6<sup>th</sup> stands "the defect detector stands". In general any stand could be mentioned as the defect detector. In addition usually just one stand could be used as the defect detector, because any vibration in stands, affects downstream stands by changing interstand tension, and affects upstream stands both by the change in the interstand tensions and the strip thickness. Actually these two parameters fluctuate with the same frequency as the defect and consequently vibrate other stand with that frequency. It means that all the vibration frequencies could be detected in all the stands. But as the largest vibration amplitude due to a defect is expected to occur on the stand that contains the defect or its neighbors. Therefore it is better to choose two or three defect detectors to determine defect on a stand. It is recommended to use other stands as the verifier just like the stand number 7 is used here.

### 4.3. Error sources

It is important to note that the formulation and defect detection procedure presented above have some approximations and simplified assumptions that affect the results. Some of the important error sources are; linearization of the stand stiffness and process parameters, simplifications on material constitutive, simplifications on mathematical expression of the defects, neglecting elastic deformation of the roll surfaces that affect the frequency of the vibrations and neglecting strip slip and stand horizontal vibration. Despite of the above mentioned error resources few percent errors in final results of defect frequency and amplitude were observed that show the ability of proposed method for industrial application where fluctuation amplitude in force and displacements are small.

### 5. Conclusion

Forced vibration of a general seven stands hot strip rolling mill due to forming rolls defects such as ovality and eccentricity was simulated successfully based on a new dynamic model. The model is established according to the Hu's cold rolling model [14]. The proposed model is adopted for hot strip rolling to be able to undertake the material strain rate effects. Results of simulation have an acceptable accordance to the data recorded in an industrial data logger. Despite the deep defects can activate the nonlinearities in the model, for the usual small defects on the work rolls and backup rolls which are in the order of few microns, the frequencies of the rolling force fluctuations derived from the simulation are identical with the theoretical characteristic frequencies. An industrial 7 stands hot strip rolling mill in MSC was analyzed with this method. Defects of 20 to 65 micrometer in the type of eccentricity or ovality were detected in work rolls and back up rolls.

It is shown that the defects on a certain stand will lead to vibration in all the stands, which is due to interstand tension and mass transfer. Regularly closer the defect to the stand leads to the larger the rolling force fluctuation amplitude.

### 6. Acknowledgment

The authors wish to thank Mobarakeh Steel Co. for cooperation and financial support of this research.

### References

1. Hu PR. Stability and chatter in rolling, PhD Thesis, Northwestern University, Evanston, 1998.
2. Orowan E. The calculation of roll pressure in hot and cold flat rolling. Proc Inst Mech Engrs, 1943; 150(4): 140 – 167.
3. Bland DR and Ford H. Cold rolling with strip tension – Part III: an approximate treatment of the elastic compression of the strip in cold rolling. Iron and Steel Institute, 1952; 171: 245 – 249.
4. Bland DR and Sims RB. A note on the theory of rolling with tensions. Proc Inst Mech Engrs, 1953; 167: 371 – 372.
5. Sims RB. Calculation of roll force and torque in cold rolling by graphical and experimental methods. Iron and Steel Institute, 1954 September; 178: 19 – 34.
6. Sims RB. Calculation of roll force and torque in cold rolling by graphical and experimental methods. Iron and Steel Institute, 1954 September; 191 – 200.

7. Alexander JM. On the theory of rolling. Proc R Soc London, 1972: 535 – 555.
8. Christensen P, Everfelt H and Bay N. Pressure distribution in plate rolling. Annals of CIRP, 1986; 35:141 – 146.
9. Gunasekera JS and Alexander JM. Analysis of rolling. Annals of CIRP, 1987; 36:203 – 206.
10. Lalli LA. An analytical rolling model including through thickness shear stress distributions. ASME J Engineering Materials & Tech, 1984; 106:1 – 8.
11. Venter R and Abd-Rabbo A. Modeling of the rolling process-I. Int J Mech Sci, 1980; 22: 83 – 92.
12. Freshwater IJ. Simplified theories of flat rolling-I: The calculation of roll pressure, roll force and roll torque. Int J Mech Sci, 1996; 38(6): 633 – 648.
13. Tlustý J, Critchley S and Paton D. Chatter in cold rolling. Annals of CIRP, 1982; 31: 195 – 199.
14. Hu PR and Ehmann KF. A dynamic model of the rolling process Part I: Homogeneous model. Int J Machine Tools & Manufacture, 2000; 40: 1 – 19.
15. Yan XQ, Sun ZH and Chen W. Vibration control in thin slab hot strip mills. Ironmaking & Steelmaking, 2011; 38(4):309-313.
16. Yildiz SK, Forbes JF, Huang B, Zhang Y, Wang F, Vaculik V and Dudzic M. Dynamic modeling and simulation of a hot strip finishing mill. Applied Mathematical Modelling, 2009; 33(7): 3208 – 3225.
17. Fan XB, Zang Y and Wang HG. Research on hot rolling mill horizontal vibration. Kang T'ieh/Iron and Steel, 2010; 45(9): 62 – 66.
18. Fan XB, Zang Y and Wang HG. Research on hot rolling mill horizontal vibration. Kang T'ieh/Iron and Steel, 2010; 21(15): 1801 – 1804.
19. Yarita I and Urukawa K. An analysis of chattering in cold rolling of ultrathin gauge steel strip. Trans Iron and Steel Inst of Japan, 1978; 18: 1 – 10.
20. Chefnieux L, Fischbach JP and Guozou J. Study and control of chatter in cold rolling. Iron and Steel Engineer, 1984; 17 – 26.
21. Sun JL, Peng Y, Liu HM and Jiang GB. Forced transverse vibration of rolls for four-high rolling mill. Journal of Central South University of Technology, 2009; 6: 16.
22. Lu YW, Zhang H, Xiong SB and Wang RF. Hot rolling mill vibration analysis based on least squares method. Journal of North University of China, 2009; 30(1): 41 – 45.
23. Yan XQ, Cao X and Liu LN. Simulation research on exceptional vibration of mill main drive system. Journal of System Simulation, 2009; 21(11,5): 3439 – 3442, 3459.
24. Forouzan MR, Salehi I and Adibi-sedeh AH. A comparative study of slab deformation under heavy width reduction by sizing press and vertical rolling using FE analysis. Journal of Materials Processing Tech, 2009; 209(2): 728 – 736.
25. Shida S. Empirical formula of flow stress of carbon steels resistance to deformation of carbon steels at elevated temperature. 2<sup>nd</sup> report, J.JSTP, 1969; 10: 610 – 617.
26. Misaka Y and Yoshimoto T. Formulation of mean resistance of deformation of plain carbon steel at elevated temperature. J of Jpn Soc of Technol of Plast, 1967-1968; 8: 414 – 442.